Initial Results for Nano-Indentation Simulations in Uintah-MPM

Jim Guilkey

University of Utah, Department of Mechanical Engineering

Abstract

In support of experimental nano-indentation measurements being made at ARL-Adelphi, analogous numerical simulations have been carried out in an attempt to give insight to the experimental results. The very first simulations done attempted to match the experimental conditions, including a "cube-corner" indentor, and an elastic-plastic with linear hardening specimen. The force required to push the diamond indentor into the specimen was recorded and plotted. While the simulations ran successfully, interpretation of the data is challenging. In an attempt to better understand the results, a series of simpler simulations were run, including different indentor shapes and test specimens that were elastic and some that were elastic-perfectly plastic. This report briefly describes those tests and the results, with the goal of better understanding the results for these simpler situations, thereby preparing all involved to interpret the more complex results in the future. Functional agreement with the expected reaction force is demonstrated as well.

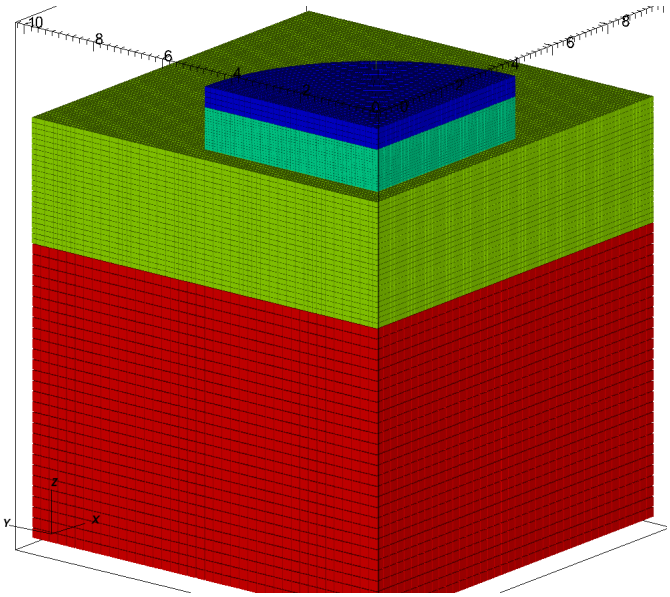

Figure 1: Initial configuration for the constant area indentor case. In this case, a quarter symmetry model was appropriate. Particles are scaled to show the resolution with which the objects are represented. Particle color indicates as follows: Blue is the rigid piston, teal is the diamond indentor, green and red are the silicon sample material, where the particles shown in red are simply larger (lower particle density) for computational efficiency.

1 Simulation Geometries and Boundary Conditions

1.1 Simulation Geometry

In this report, only the simplified cases will be described. For each, a small elastic specimen has a free top surface and is bounded by planes of symmetry on all other surfaces (bottom and sides). The specimen has elastic properties approximating silicon, while the indentor has elastic properties approximating diamond (much stiffer). The diamond indentor is pushed by a rigid piston for which the displacement is controlled. Separate indentor and piston materials were used so that the friction contact algorithm in Uintah could be used to goven the interaction between the indentor and specimen. Specifically, this contact algorithm turns off the contact constraint once there is no longer a normal traction representing compression between two materials, and their relative velocities are no longer toward each other.

Initial configurations for the three cases under consideration are shown in Figures 1-3. These graphics show the initial particle representation. Particles are underscaled, slightly, to illustrate the resolution with which the objects are represented. Dark blue particles represent the rigid piston, teal (or light green) particles are the diamond indentor, while the lime green and red particles are the specimen. Red particles are the same material, just represented at a lower resolution to save computational time away from the interaction zone. Figure1 shows a constant area indentor, the cube-corner indenter in Figure 2 has a cross-sectional area that varies as the square of the depth of penetration, while Figure 3 depicts a cube-edge indentor, the cross-sectional area of which increases linearly with depth of indentation.

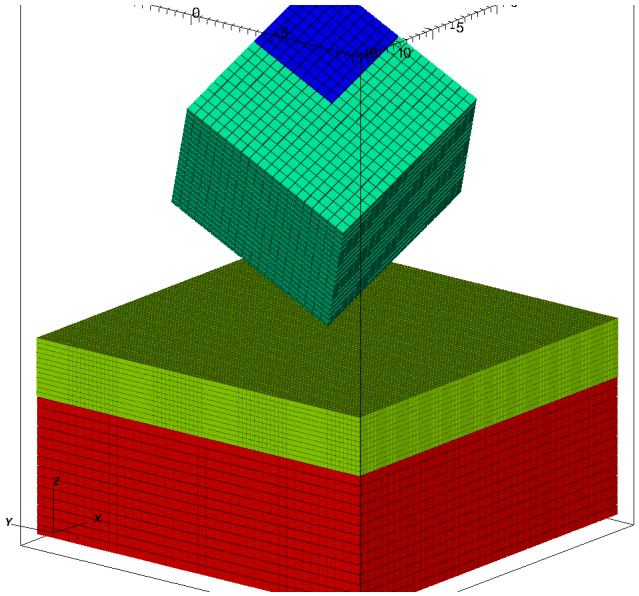

Figure 2: Initial configuration for the cube-corner indentor case. Here, the cross sectional area of the indentor increases quadratically with depth of penetration. Particles are scaled to show the resolution with which the objects are represented. Particle color indicates as follows: Blue is the rigid piston, teal is the diamond indentor, green and red are the silicon sample material, where the particles shown in red are simply larger (lower particle density) for computational efficiency.

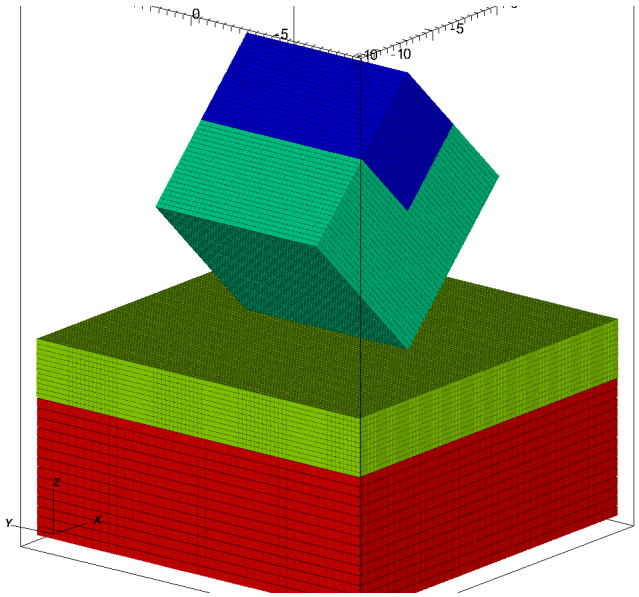

Figure 3: Initial configuration for the constant area indentor case. In this case, a quarter symmetry model was appropriate. Particles are scaled to show the resolution with which the objects are represented. Particle color indicates as follows: Blue is the rigid piston, teal is the diamond indentor, green and red are the silicon sample material, where the particles shown in red are simply larger (lower particle density) for computational efficiency.

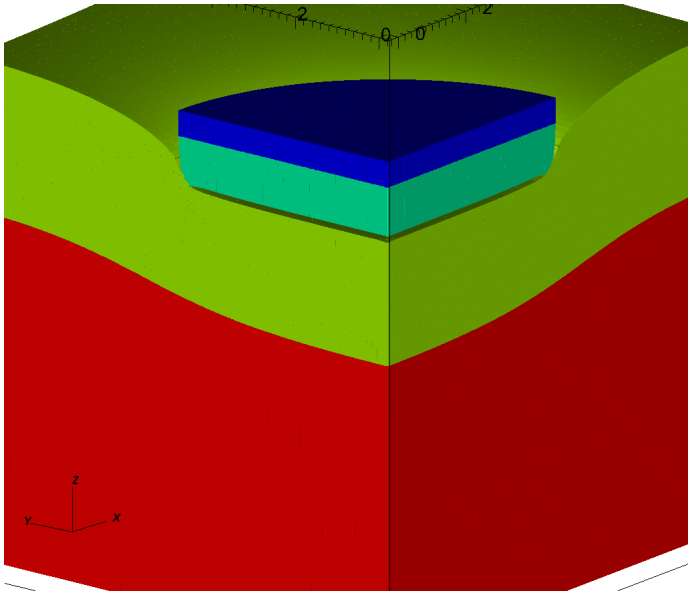

Figure 4: Constant area configuration at full indentation.

1.2 Boundary Conditions

The boundary conditions on all but the top surface of the specimen are symmetry planes. The piston is given a constant velocity downward (-10 nm/nanosecond) for 2 nanoseconds at which time the piston is briefly stopped and reversed. This results in a 20% indentation into the 100 nm thick sample.

2 Elastic Results

Here we describe the results for elastic samples, first with a depiction of the geometry, followed by graphs of the force on the indentor.

2.1 Indented Geometry

Figures 4-6 depict the particle configuration at maximum penetration, which is 20% of the thickness of the sample (maximum depth of the penetrator).

2.2 Reaction Force Plots

A feature of the rigid contact algorithm is the output of the resultant force that the rigid object experiences. This can be thought of as the force required to maintain the velocity assigned to that object. Figures 7-9 contain plots of the force on the y-axis and time on the x-axis. Time could be converted to indentor displacement very simply, and eventually will be, but for the purpose of this report, the independent variable will remain time.

For the constant area indentor, the force vs. time plot looks very much as one would expect. The force magnitude increases linearly until the piston stops, and then during

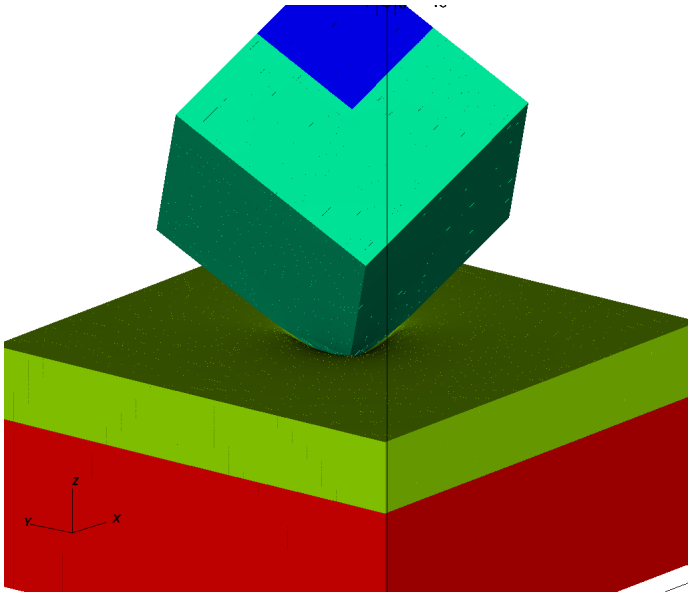

Figure 5: Quadratic area configuration at full indentation.

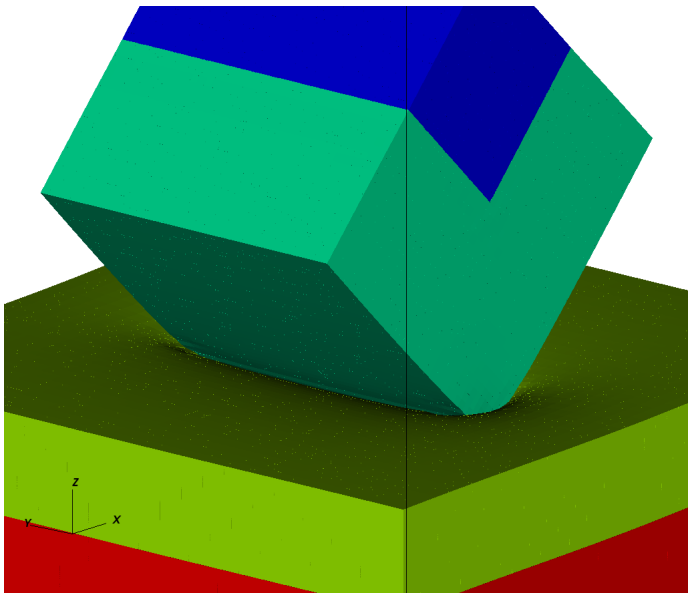

Figure 6: Linear area configuration at full indentation.

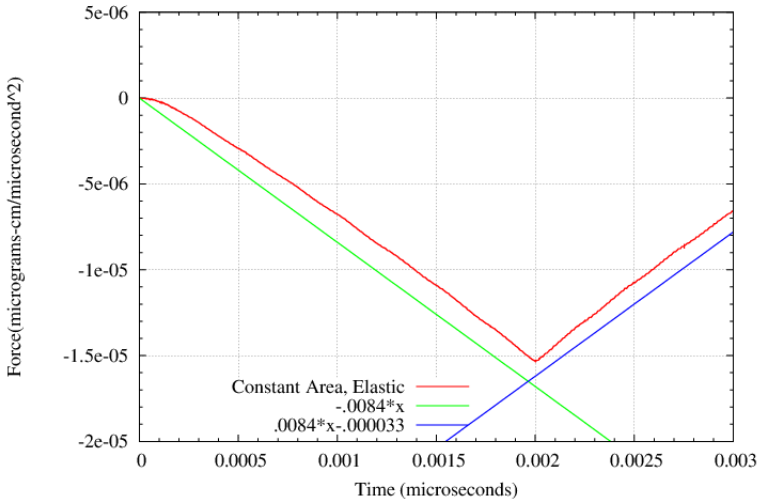

Figure 7: Constant area configuration at full indentation. Analytical expressions are approximate fits only.

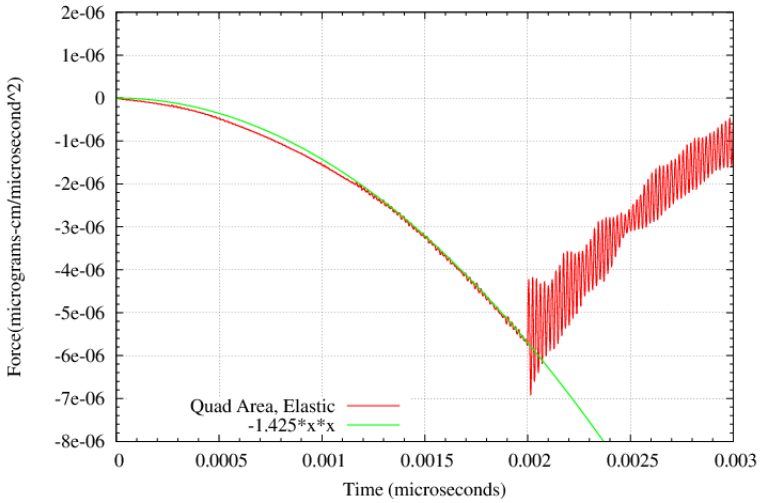

Figure 8: Quadratic area configuration at full indentation. Analytical expression is an approximate fit to the loading portion of the data.

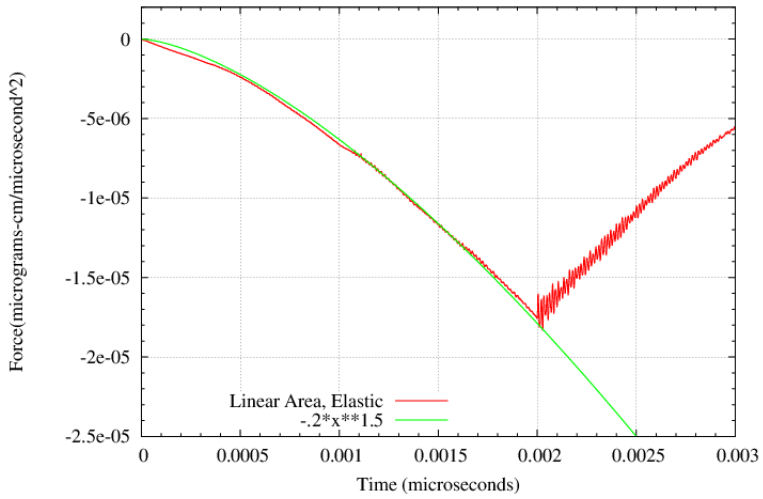

Figure 9: Linear area configuration at full indentation. Analytical expression is an approximate fit to the loading portion of the data.

unloading, the force magnitude decreases with the same slope, again, as expected.

(For the next two plots, there is significant noise in the unloading. I have a couple of suspicions as to what may be causing this, and this will eventually be resolved. For the sake of the discussion here, the unloading portion of the curve can be ignored.) For the cube-corner indentor, the cross-sectional area of indentor that is in contact with the sample goes up as the square of the depth of indentation. Figure 8 includes an approximate fit to the data (green curve) shows that the force magnitude is quadratically dependent on penetration depth during loading.

This result motivated the final configuration, in which the cross sectional area of the indentor that is in contact with the sample increases linearly with depth of penetration. There, in Figure 9, an approximate fit to the data is again drawn in green. This time, the force magnitude increases as time (depth) to the 3/2 power.

2.3 Expected Functional Form

Based on a lack of experience, the author had no solid expectations of the functional form of the force experienced by the indentor. However, the nano-indentation Wikipedia page (https://en.wikipedia.org/wiki/Nanoindentation) revealed:

$$E_r = \frac{1}{\beta}\frac{\sqrt{\pi}}{2}\frac{S}{\sqrt{A_p(h_c)}} \tag{1}$$

where E_r is the "reduced Young's Modulus" of the test specimen, β is an order 1 geometric constant, $A_p(h_c)$ is the projected area of the indentor at depth h_c. S is the stiffness and is proportional to the slope of the unloading curve, $\frac{dP}{dh}$. Rearranging this, we have:

$$S = \frac{2E_r\beta}{\sqrt{\pi}}\sqrt{A_p(h_c)} \tag{2}$$

Consider each of the three cases in light of Eq. 2. For the constant area case, $A_p(h_c)$ is a constant, and the slope of the loading (and unloading) curve is a constant. For the cube-corner indentor, $A_p(h_c) = 2.598h^2$, so we expect the slope of the unloading curve to vary linearly with penetration, which it does (Figure 8). Finally, for cube-edge indentor, $A_p(h_c) = k_1 h$, and $P = k_2 h^{3/2}$ (Figure 9, so $\frac{dP}{dh} = 3/2k_2 h^{1/2}$. Thus, for each of the cases considered, simulations are returning the expected functional form of the force vs. indentation curve.

3 Discussion

Now that we have demonstrated that Uintah simulations generate results of the expected functional form for loading, we are nearly ready to move to more complex material response. Because moving to plasticity will require using the unloading portion of the curve, resolving the noise during unloading will be necessary. We also need to translate the time domain currently used on the horizontal axis to an indentation, and ensure that we can extract a reliable value of Young's modulus for the specimen. At that point, we will feel confident in our methods and will be able to move to more complicated material response.